

MECHANICAL SYSTEM OF THE U26 UNDULATOR PROTOTYPE FOR SHINE

S. W. Xiang, T. T. Zhen[†], S. D. Zhou, Y. Y. Lei, J. Yang, W. Zhang, Z. Q. Jiang,
 R. B. Deng, H. X. Deng

Shanghai Advanced Research Institute, Chinese Academy of Sciences, Shanghai, China

Abstract

The Shanghai High repetition rate XFEL and Extreme light facility (SHINE) is under construction and aims at generating X-rays between 0.4 and 25 keV with three FEL beamlines at repetition rates of up to 1 MHz. The three undulator lines of the SHINE are referred to as the FEL-I, FEL-II, and FEL-III. Shanghai Synchrotron Radiation Facility (SSRF) will manufacture a total of 42 undulators (U26) with a period length of 26 mm for FEL-I and 22 undulators (U55) with a period length of 55 mm for FEL-II. Both the U26 and U55 are 4 m long and use a common mechanical system. By using the specially designed double lever compensation springs can eliminate different magnetic force on the drive units. A U26 prototype has been developed and tested at SSRF. This paper describes the mechanical system design, simulation and testing results of the U26 prototype, as well as its compatibility with U55.

INTRODUCTION

SHINE has three undulator lines [1-3], with FEL-I and FEL-II arranged side by side in the same tunnel, as shown in Fig. 1. Due to space limitations, the vacuum chamber needs to be installed and aligned on the undulator frame outside the tunnel. The width of the undulator is 1.1 m, and the transportation access space is 1.5 m to ensure that the undulator can be transported normally.

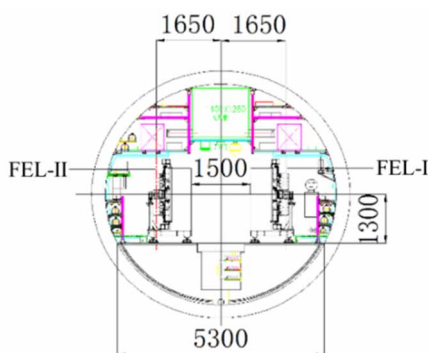


Figure 1: Cross section of the SHINE undulator tunnel.

MECHANICAL SYSTEM DESIGN

Considering that both U26 and U55 are 4 meters long, the mechanical system will be the same, but the magnetic structures will be different. The mechanical system is composed of a L-shape steel frame, girders, drive units, compensation springs, and alignment jacks, as illustrated in



Figure 2: SHINE U26 prototype mechanical system.

Fig. 2. The function of the mechanical system is to support and drive the upper and lower girders with magnet structures to move symmetrically relative to the magnetic center. Mechanical tolerances are determined by FEL physics, and the main parameters of the mechanical system are listed in Table 1.

Table 1: Main Parameters of the Mechanical System

Parameter	Value	Unit
Maximum gap range	7-200	mm
Nominal gap range	7-14@U26	mm
	7-30@U55	
Maximum magnetic force	26@U26	kN
	65@U55	
Gap variation under maximum magnetic force	≤10@U26	μm
	≤20@U55	
Gap drive repeatability	±1	μm
Taper range	±0.2	mm
Moving range of the magnetic center	±0.4	mm

The frame is a welded steel structure supported by a set of six jacks for leveling and alignment. The drive units adopt four motors to adjust the gap and the taper, and consists of motors, gearboxes, lead screws, linear guides, limit switches, hard stops, and encoders. In order to improve the rigidity of the girder, hardened and tempered 42CrMo forging are selected. The double lever compensation springs (DLCS) is composed of two sets of disc springs with different stiffness, as shown in Fig. 3. It is installed between the upper and lower support plates, which can eliminate the magnetic force on the drive units.

[†] email address: zhentt@sari.ac.cn

Content from this work may be used under the terms of the CC-BY-4.0 licence (© 2023). Any distribution of this work must maintain attribution to the author(s), title of the work, publisher, and DOI

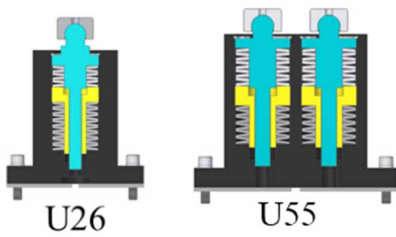


Figure 3: Double lever compensation springs.

GAP VARIATION ANALYSIS AND MEASURES

The upper and lower girders will deform under the magnetic force, resulting in the gap variation. The magnitude magnetic field. The results of gap variation measured by laser displacement meters are consistent with the Finite Element Analysis (FEA), as shown in Fig. 4. Under the magnetic force of 26 kN, the maximum gap variation of U26 is close to 8 μm as shown in Fig. 5. The phase angle measured is within 6° , which meets the physical requirements. Adjust the minimum gap of U26 to 4.6 mm, which can be equivalent to simulating the maximum magnetic force 65 kN of U55. The maximum gap variation of U55 is close to 18 μm as shown in Fig. 6, which also meets the requirement in specification.



Figure 4: Gap variation measurement.

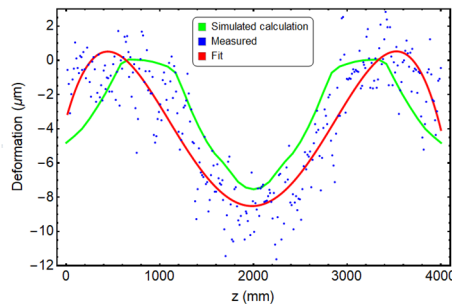


Figure 5: Maximum gap variation of U26.

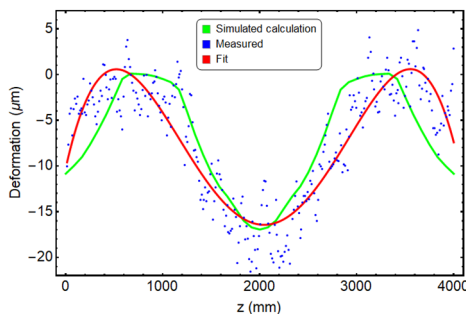


Figure 6: Maximum gap variation of U55.

SPRING CURVES MEASURED AND FATIGUE TEST

The compensation springs adopt the double lever structure, mainly used to eliminate the magnetic force on the drive units. The theoretical spring force curve is nonlinear and should be as close as possible to the magnetic force curve. Actual spring force curves of U26 and U55 were measured by an electric servo testing machine, as shown in Figs. 7 and 8. At the minimum gap of 7 mm, the spring force measured value of U26 is 28000 N, slightly higher than the theoretical value of 25000 N, with an error of 12%. At the minimum gap of 7 mm, the spring force measured value of U55 is 64700 N, slightly lower than the theoretical value of 65436 N, with an error of 1.2%. The results showed that the measured curve basically coincides with the theoretical curve.

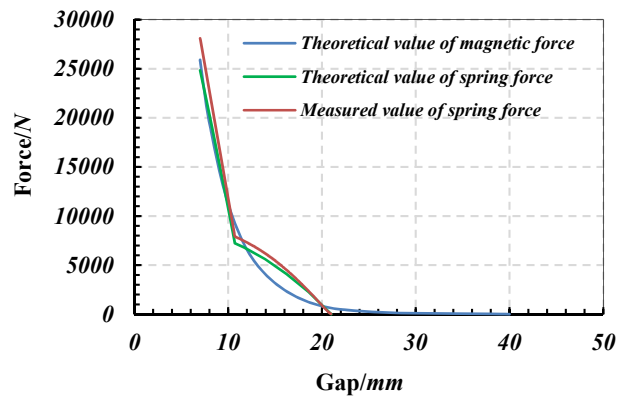


Figure 7: Magnetic and spring force curves of U26.

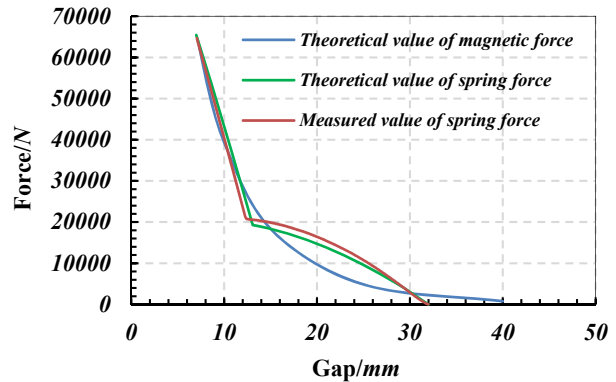


Figure 8: Magnetic and spring force curves of U55.

The long-term operation of compensation springs may cause significant changes in the spring force or structural fatigue damage due to friction, thereby affecting magnetic field stability. 5000 times fatigue tests were conducted on the compensation springs of U26 and U55 respectively. The results are shown in Figs. 9 and 10. It can be found that the movement is smooth, and the spring force curve basically coincides. Multiple movements lead to wear between the guide rod and the disc spring, resulting in a change in spring force of less than 7%, which can be ignored in terms of its impact on magnetic field performance.

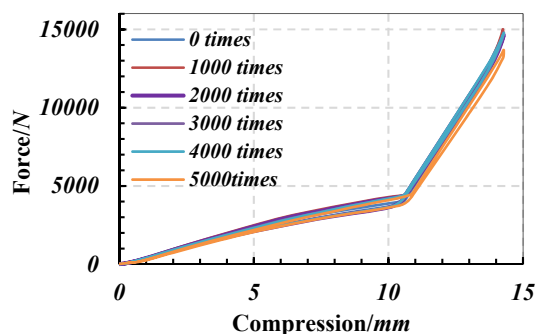


Figure 9: Spring fatigue test of U26.

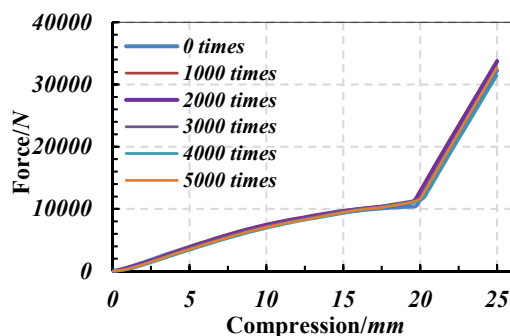


Figure 10: Spring fatigue test of U55.

The load reduction effect of the DLCS is ultimately verified by the control system reading the maximum output torque of the motor, as shown in Table 2. The results show that the magnetic force applied to the drive units has been eliminated by DLCS, and the output torque is mainly determined by gravity, friction, and inertial force.

Table 2: U26 Output Torque of the Motor (unit: nm)

Direction of motion	Position	without DLCS	with DLCS
7 mm→	upper girder 1	1.2	0.7
	upper girder 2	1.2	0.7
	lower girder 1	0.6	0.2
	lower girder 2	0.6	0.2
30 mm→	upper girder 1	0.5	0.35
	upper girder 2	0.5	0.35
	lower girder 1	0.9	0.9
	lower girder 2	0.75	0.75

LIFTING ANALYSIS AND TEST

All undulators will be tested in laboratory, to qualify their performance in the tunnel, it is necessary to ensure the structure does not occur irreversible deformation during lifting. The undulator adopts a three-point lifting method, with the lifting point located at the bottom of the frame and as close as possible to the three main support points of the undulator, which can effectively reduce the deformation caused during the process from standing to lifting, as shown in Fig. 11. Through finite element analysis, it is found that the maximum stress occurs at the front lifting

point, which is 38 MPa much less than the yield strength of Q345. By measuring the magnetic field before and after lifting, the phase error variation caused by lifting is within a range of 1°, meeting the physical requirements, as shown in Fig. 12.



Figure 11: Lifting method and stress FEA results.

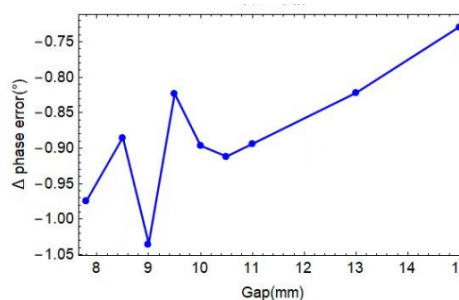


Figure 12: Phase error variation caused by lifting.

CONCLUSIONS

For the FEL-I at the SHINE a U26 prototype has been built and tested by SSRF, China. The measured performance parameters of the U26 prototype satisfy the technical requirements and are basically consistent with the design and simulation results. The mechanical system of U26 has been verified to be equally applicable to U55, which is beneficial for reducing equipment types and shortening research and development cycles.

ACKNOWLEDGEMENTS

This work was supported by the CAS Project for Young Scientists in Basic Research (YSBR-042), the National Natural Science Foundation of China (12125508, 11935020), Program of Shanghai Academic/Technology Research Leader (21XD1404100), and Shanghai Pilot Program for Basic Research - Chinese Academy of Sciences, Shanghai Branch (JCYJ-SHFY-2021-010).

REFERENCES

- [1] Z. T. Zhao *et al.*, “SCLF: an 8-GeV CW SCRF linac-based X-ray FEL facility in Shanghai”, *Proceedings of the FEL2017*. Santa Fe, NM, USA, 2017. doi:10.18429/JACoW-FEL2017-MOP055
- [2] Z. T. Zhao, C. Feng, K. Q. Zhang, “Two-stage EEHG for coherent hard X-ray generation based on a superconducting linac”, *Nucl. Sci. and Tech.*, vol. 28, p. 117, 2017. doi:10.1007/s41365-017-0258-z
- [3] C. Feng, H. X. Deng, “Review of fully coherent free-electron lasers”, *Nucl. Sci. and Tech.*, vol. 29, p.160, 2018. doi: 10.1007/s41365-018-0490-1